

Communication

^{15}N chemical shift anisotropy in protein structure refinement and comparison with NH residual dipolar couplings

Rebecca S. Lipsitz and Nico Tjandra*

Laboratory of Biophysical Chemistry, Building 50, Room 3503, National Heart, Lung, and Blood Institute, National Institutes of Health, Bethesda, MD 20892-8013, USA

Received 10 March 2003; revised 8 May 2003

Abstract

Recent methods of aligning proteins which were developed in order to measure residual dipolar couplings (RDCs) in solution can also be used for additional applications such as measuring the ^{15}N CSA in the form of chemical shift differences, $\Delta\delta$. A new XPLOR-NIH module has been developed and implemented for NMR structure refinement using the ^{15}N $\Delta\delta$ data as restraints. The results of this refinement are shown using the protein Bax. This method should be amenable to any protein which can be studied by NMR. An analysis comparing the structural information provided by NH RDCs and the ^{15}N $\Delta\delta$ is included. Published by Elsevier Science (USA).

Keywords: Chemical shift anisotropy; Residual dipolar coupling; Protein structure refinement

1. Introduction

The ^{15}N CSA is very sensitive to the local electronic and molecular environment and therefore represents a powerful tool with which to characterize protein structure and interpret relaxation data [1,2]. However, most ^{15}N CSA measurements are done on single crystals which can be difficult to obtain or on powder samples, in which case the exact orientation of the ^{15}N CSA tensor is difficult to interpret independent of other data such as tensor orientation information from analogous compounds or ab initio calculations. Furthermore it is usually near impossible to get ^{15}N CSA data for more than a few specific sites within a protein. Previous ^{15}N CSA measurements done in the solution state have been obtained from cross-correlation data between the ^{15}N – ^1H dipolar and ^{15}N CSA interactions [3,4], relaxation data at several different field strengths [5,6], and measurements in bicelle media [7,8]. Here we employ a straightforward method conceptually similar to that of Boyd and Redfield [7] for obtaining ^{15}N chemical shift orientation-dependent differences ($\Delta\delta$) in a solution

environment using magnetically aligned protein samples in solution and demonstrate how this information can be applied towards structure refinement. There have been many papers published previously where chemical shifts, particularly ^1H chemical shifts, are used for NMR structure refinement [9,10] but the present technique differs markedly from those protocols. In the previous studies the calculated chemical shifts are usually a function of variables that require parameterization whereas in this situation, it is changes in chemical shift due to partial alignment that are being used as restraints and the variables needed to calculate the ^{15}N chemical shifts are based on experimentally determined values. The magnetically aligned sample conditions used here are the same as those used for obtaining NH residual dipolar couplings (RDCs) [11,12]. One important point that must be emphasized is that the ^{15}N $\Delta\delta$ data, which is a direct manifestation of the ^{15}N CSA, is complementary to NH RDCs, yet provides a unique source of structural information. In this paper, the apoptosis protein Bax [13] is used to demonstrate these techniques.

In order to measure the ^{15}N $\Delta\delta$ data, the ^{15}N chemical shifts were recorded under isotropic and anisotropic conditions using a HNCOC experiment as demonstrated for $^{13}\text{C}'$ $\Delta\delta$ data [14]. Both the isotropic and anisotropic

* Corresponding author. Fax: 1-301-402-3404.

E-mail address: nico@helix.nih.gov (N. Tjandra).

samples were the same (0.5 mM proteins, 10 mM Tris-acetate, 2 mM DTT, pH 6.0, 305 K). In order to create the anisotropic environment, Pfl phage particles were added (12 mg/ml) [15]. Fig. 1 shows the overlay of the isotropic and anisotropic data for residue Gly 160. In this particular HNCO experiment there is no decoupling in the ^{15}N dimension and therefore the ^{15}N doublet is retained [16]. PIPP software was used to analyze the data [17]. The chemical shifts were determined using contour averaging [18] under both sets of solution conditions. The actual ^{15}N chemical shift is taken as the average of the two doublet components. Constant time evolution was used in the ^{15}N dimension with an acquisition time of 27.2 ms. The error of the measurement was 0.4 Hz which is based on the assumption that the reproducibility of the error of the ^{15}N chemical shift is approximately twice that of the ^{13}C chemical shift [19]. This is reasonable given that a comparable acquisition time along with similar data processing and analysis for the protein ubiquitin, which is roughly half the size of Bax, resulted in an error of reproducibility of 0.15 Hz [20].

The method introduced in this paper relies on the ability to measure chemical shifts with relatively good precision. The limits of this method are that all peaks are well resolved and the error in the measurement is at least an order of magnitude smaller than the spread in $\Delta\delta$ values. In the three-dimensional HNCO nearly all peaks were well-resolved. Bax is a moderate size protein of 192 residues but incorporation of TROSY methods into the HNCO experiment could be used for larger proteins where spectral resolution becomes problematic [21]. The range of ^{15}N $\Delta\delta$ values for Bax is approximately 200 ppb which is an order of magnitude larger than the error in the ^{15}N $\Delta\delta$ values, 17 ppb, a value that accounts for the error in the ^{15}N chemical shift measurement, structural noise, and site to site variations in the ^{15}N CSA tensor [19]. The error should be similar for larger proteins as long as there is no significant spectral overlap.

One of the major advantages of measuring the ^{15}N chemical shift changes in the solution state is that the

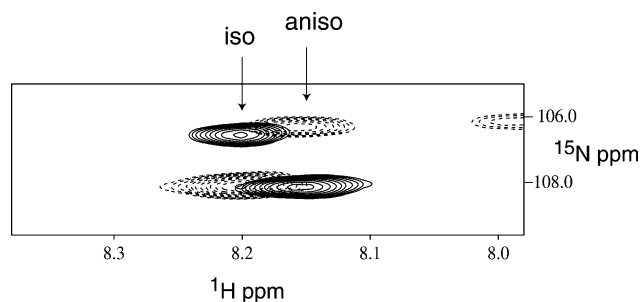


Fig. 1. ^{15}N $\Delta\delta$ data for Gly 160 from an HNCO experiment. The ^{15}N $\Delta\delta$ is the difference between the average of the two isotropic peaks and the two anisotropic peaks.

data are available for every residue in the protein (except prolines) and can be used for structure refinement. In order to carry out the refinement a new module was incorporated into the program XPLOR-NIH [22]. The refinement is based on comparing the experimentally derived and calculated ^{15}N $\Delta\delta$ values from the starting structure according to the following equation:

$$\Delta\delta = \sum_{i=x,y,z} \sum_{j=x,y,z} A_{jj} \cos^2 \theta_{ij} \delta_{ii}, \quad (1)$$

where A_{jj} is the principal axis of the molecular alignment tensor, δ_{ii} is the principal axis of the traceless CSA tensor, and θ_{ij} is the angle between A_{jj} and δ_{ii} . The $\Delta\delta$ values are a reflection of the ^{15}N CSA tensor properties as well as its orientation in the alignment frame. In the XPLOR-NIH refinement, the following energy term is generated according to the difference between the experimentally measured and the calculated ^{15}N CSA values:

$$E_{\text{CSA}} = k_{\text{CSA}} (\Delta\delta_{\text{obs}} - \Delta\delta_{\text{calc}})^2, \quad (2)$$

where k_{CSA} is the force constant used in the MD simulations. Values for the magnitudes of the principal components of the diagonalized traceless CSA tensor, the initial value of the force constant, and the final value of the force constant must be specified. Previously determined values were used for the magnitude of the ^{15}N CSA tensor principal axis components ($\sigma_{11} = 108.5$, $\sigma_{22} = -45.7$, $\sigma_{33} = -62.8$) [19]. The force constant values used were determined empirically in such a way that the final rmsd of the ^{15}N $\Delta\delta$ was equal to 17 ppb. The initial force constant value was 0.0001 kcal/ppb² which was increased to a final value of 0.003 kcal/ppb². Fig. 2a shows the improved correlation between the observed ^{15}N $\Delta\delta$ values prior to and after refinement. In order to validate the results of the ^{15}N $\Delta\delta$ refinement the structures were calculated without the $\text{C}_\alpha\text{-H}_\alpha$ RDCs in order to use them as a gauge of structural improvement. Fig. 2b shows the improvement between the observed and calculated $\text{C}_\alpha\text{-H}_\alpha$ RDCs upon inclusion of the ^{15}N $\Delta\delta$ restraints. The correlation coefficient, R , changes from 0.853 to 0.884.

The energy terms and rmsd values for Bax structures refined with the ^{15}N $\Delta\delta$ protocol are shown in Table 1. For comparison, results are also listed for structures calculated without NH RDC or ^{15}N $\Delta\delta$ restraints, structures calculated with NH RDC restraints but without ^{15}N $\Delta\delta$ restraints, and structures calculated with ^{15}N $\Delta\delta$ restraints but without NH RDC restraints. Thirty structures were calculated for each set of parameters and the average values from the 10 lowest energy structures are included in the table. Looking at the rms values for the NH RDCs and the ^{15}N $\Delta\delta$ it can be seen that inclusion of the ^{15}N $\Delta\delta$ restraints alone considerably improves the NH RDCs. However, the reverse is not true; inclusion of the NH RDCs alone only has a

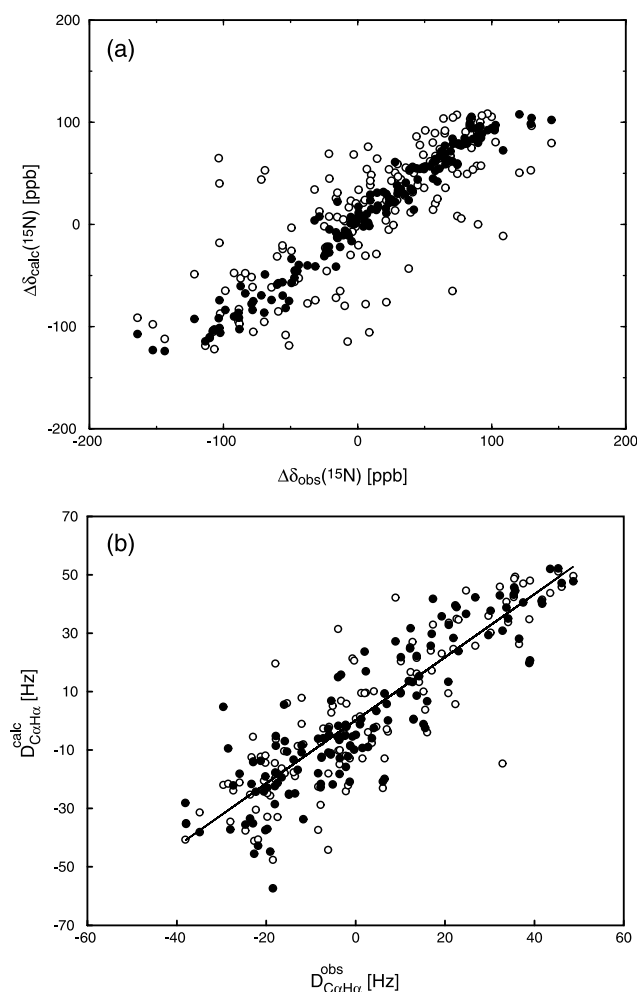


Fig. 2. (a) Data showing the correlation between the observed and calculated ^{15}N $\Delta\delta$ for Bax before (○) and after (●) ^{15}N CSA refinement. (b) The D_{CH} values before (○) and after (●) ^{15}N refinement, in both cases without inclusion of D_{CH} restraints.

modest impact on the ^{15}N $\Delta\delta$ rms. However, in both cases there is an improvement in the structural convergence compared to the structures refined without NH RDCs or ^{15}N $\Delta\delta$ as judged by the backbone and heavy atom rmsd values.

Although the ^{15}N $\Delta\delta$ and the NH RDCs both provide orientation information on the ^{15}N backbone nuclei the nature of this information is distinct. This is illustrated in Fig. 3 which compares Leu 15 and Ile 23. The angles used to determine the position of σ_{xx} , σ_{yy} , σ_{zz} relative to the peptide plane are taken from a previous study [19]. These two residues have the same NH RDC and therefore the same orientation of the NH bond vector with respect to molecular alignment frame. However, the orientations of the principal components of the ^{15}N CSA tensor are unique and as a result, so are the ^{15}N $\Delta\delta$ values. If the information provided by ^{15}N $\Delta\delta$ values is duplicated by that of the NH RDCs, one would instead see the same systematic difference between all values of ^{15}N $\Delta\delta$ and NH RDCs. Fig. 4 shows a plot of ^{15}N $\Delta\delta$ values vs. the NH RDCs. Clearly, the ^{15}N $\Delta\delta$ and the NH RDCs are moderately correlated. However, given that the targeted ^{15}N $\Delta\delta$ rmsd is 17 ppb and that the deviation from a perfect correlation between the ^{15}N $\Delta\delta$ and NH RDCs exceeds this amount demonstrates that there must be different contributions to the ^{15}N $\Delta\delta$ and NH RDCs.

In order to understand the differences between the ^{15}N $\Delta\delta$ and NH RDCs it is useful to consider the nature of the ^{15}N CSA. The ^{15}N CSA is sensitive to variables which can effect the degree of chemical shielding such as ϕ , ψ , and χ^1 torsion angles, hydrogen bonding, the NH bond length, the identity of nearby amino acids, and electrostatic effects [23–26]. Fig. 5 shows the NH RDC and ^{15}N $\Delta\delta$ values from a structure refined with NH RDC restraints but without any ^{15}N $\Delta\delta$ restraints. While the NH RDCs somewhat improve the correlation

Table 1
Data for Bax protein structures using ^{15}N CSA refinement

	Null refinement ^a	RDC refinement ^b	^{15}N $\Delta\delta$ refinement ^c	NH RDC and ^{15}N $\Delta\delta$ refinement ^d
Energies (kcal/mol)				
Overall	416 ± 12	465 ± 18	604 ± 9	508 ± 12
NOE	13.8 ± 3.0	14.7 ± 2.3	19.0 ± 3.5	16.4 ± 5.2
Dihedral	0.35 ± 0.18	0.32 ± 0.17	0.91 ± 0.28	0.61 ± 0.33
Vdw	74.7 ± 4.3	79.8 ± 6.4	87.6 ± 5.4	75.3 ± 5.1
rmsds				
^{15}N - ^1H RDC (Hz)	6.11 ± 0.70	1.98 ± 0.12	4.40 ± 0.17	2.44 ± 0.10
^{15}N CSA (ppb)	42.0 ± 2.2	36.6 ± 2.1	15.2 ± 0.4	13.8 ± 0.55
Structure rmsds (helical residues)				
Backbone	0.89 ± 0.11	0.77 ± 0.11	0.80 ± 0.11	0.83 ± 0.10
Heavy atom	1.63 ± 0.12	1.63 ± 0.14	1.64 ± 0.11	1.59 ± 0.10

^a Refinement without NH RDCs or ^{15}N CSA.

^b Refinement with NH RDCs, without ^{15}N CSA.

^c Refinement with ^{15}N CSA, without NH RDCs.

^d C_α - H_α RDCs omitted.

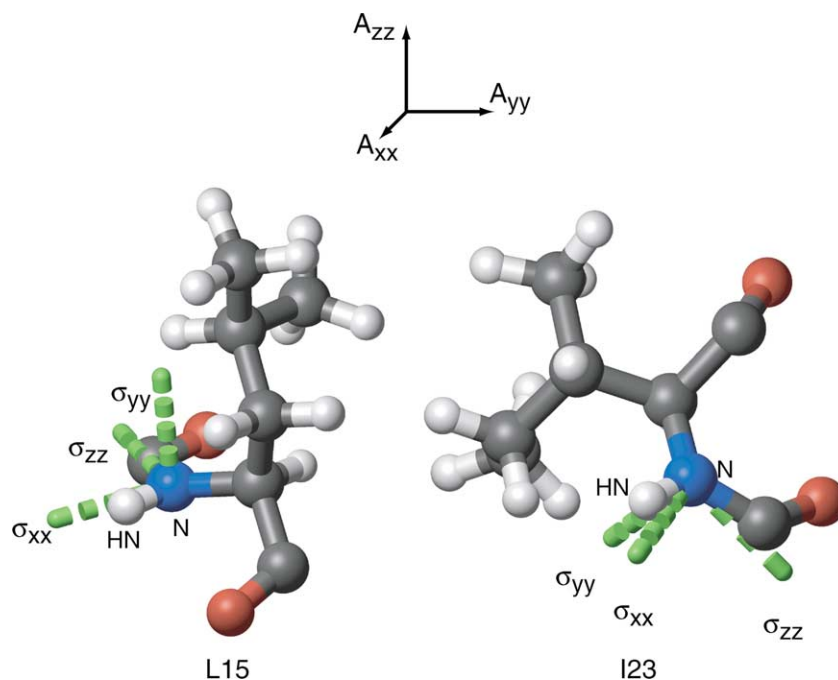


Fig. 3. The orientation in the molecular alignment frame of residues Leu 15 ($D_{\text{NH}} = 10.15 \text{ Hz}$, $^{15}\text{N } \Delta\delta = -96.2 \text{ ppb}$) and Ile 23 ($D_{\text{NH}} = 10.13 \text{ Hz}$, $^{15}\text{N } \Delta\delta = -11.30 \text{ ppb}$). The position of the backbone nitrogen and amide proton is shown along with the orientation of the three principal components of the ^{15}N CSA tensor according to Cornilescu and Bax [19].

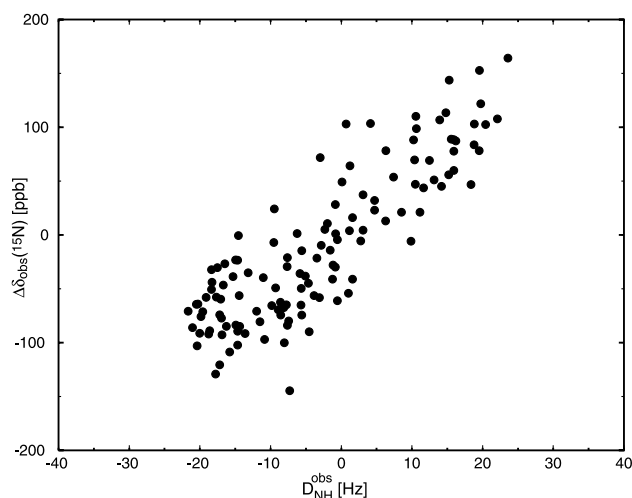


Fig. 4. The $^{15}\text{N } \Delta\delta$ vs. the NH RDCs for Bax.

between the $^{15}\text{N } \Delta\delta$ observed and calculated values, the correlation is still rather poor compared to that for the NH RDCs, again suggesting that there are additional contributions to the $^{15}\text{N } \Delta\delta$ not taken into account by the NH RDCs. This has to do with the fact that the NH RDC refinement improves the accuracy of a single vector whereas the $^{15}\text{N } \Delta\delta$ refinement reflects the geometry of the three-dimensional ^{15}N CSA tensor. While a rotation about the NH bond relative to the alignment tensor axis will not change the NH RDC value, it will significantly effect the $^{15}\text{N } \Delta\delta$ value.

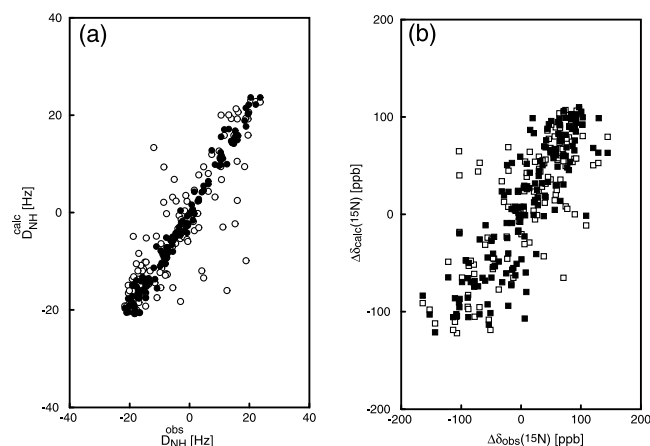


Fig. 5. Effect of D_{NH} refinement on $^{15}\text{N } \Delta\delta$ values. (a) D_{NH} values before and after refinement with correlation coefficients of $R = 0.837$ (○) and $R = 0.990$ (●). (b) $^{15}\text{N } \Delta\delta$ values for the same structure before (○) and after (●) refinement with correlation coefficients of $R = 0.777$ (□) and $R = 0.854$ (■).

There is much discrepancy as to whether or not there are residue specific differences in ^{15}N CSA tensor values; using residue-specific principal axis values may be important for interpretation of dynamics data, particularly at high magnetic fields [6]. The force constant used in the refinement to derive a final rmsd which is larger than the experimental error is meant to take into account residue-specific variations. Finally, hydrogen bonding patterns may influence the ^{15}N

CSA without affecting the NH RDC. In the case of the ^{15}N CSA it has been determined that decreases in σ_{zz} are accompanied by decreases in the hydrogen bond length, $R_{\text{N}\cdots\text{O}}$, and that σ_{xx} , and σ_{yy} may show a dependence on the hydrogen bond angle [27]. The net effect of changes in more than one of the variables thought to influence the ^{15}N CSA is even less clear. Given the complexity of the factors effecting the ^{15}N CSA and NH RDCs it is difficult to find a single parameter to which differences for a given residue can be attributed. Currently our incomplete understanding of how structural factors govern the ^{15}N CSA tensor puts a limit on how well we can refine a structure with respect to measured ^{15}N $\Delta\delta$ values. In the future when all of these various contributions to ^{15}N CSA are well understood, the ^{15}N $\Delta\delta$ refinement will only be limited to experimental error.

Previous studies on the ^{15}N CSA have produced discrepancies as to the average ^{15}N CSA value. Calculation of the protein-average ^{15}N CSA using $\Delta\delta$ requires at least five independent $\Delta\delta$ measurements for a given alignment tensor. When a complete set of high quality RDC data and NOEs data are available one can evaluate the optimal average ^{15}N CSA value by a grid search method [14] during the ^{15}N $\Delta\delta$ refinement. The optimal average ^{15}N CSA value can be better determined when ^{15}N $\Delta\delta$ values measured in different alignment media are available. In fact this protocol can be applied to substructures of the protein. This will be useful for studying the variation in the average ^{15}N CSA value and how it is correlated with conformational and structural preferences. In addition, since the CSA values are required for dynamics data fitting, this technique provides a simple method to improve accuracy in the interpretation of dynamics data.

References

- [1] N. Tjandra, A. Bax, Solution NMR measurement of amide proton chemical shift anisotropy in ^{15}N -enriched proteins. Correlation with hydrogen bond lengths, *J. Am. Chem. Soc.* 119 (1997) 8076–8082.
- [2] M. Ottiger, N. Tjandra, A. Bax, Magnetic field dependent amide ^{15}N chemical shifts in a protein–DNA complex resulting from magnetic ordering in solution, *J. Am. Chem. Soc.* 119 (1997) 9825–9830.
- [3] N. Tjandra, A. Szabo, A. Bax, Protein backbone dynamics and ^{15}N chemical shift anisotropy from quantitative measurement of relaxation interference effects, *J. Am. Chem. Soc.* 118 (1996) 6986–6991.
- [4] J.R. Tolman, J.M. Flanagan, M.A. Kennedy, J.H. Prestegard, Nuclear magnetic dipole interactions in field-oriented proteins: information for structure determination in solution, *Proc. Natl. Acad. Sci. USA* 92 (1995) 9279–9283.
- [5] D. Fushman, N. Tjandra, D. Cowburn, An approach to direct determination of protein dynamics from ^{15}N NMR relaxation at multiple fields, independent of variable ^{15}N chemical shift anisotropy and chemical exchange contributions, *J. Am. Chem. Soc.* 121 (1999) 8577–8582.
- [6] C.D. Kroenke, M. Rance, A.G. Palmer III, Variability of the ^{15}N chemical shift anisotropy in *Escherichia coli* ribonuclease H in solution, *J. Am. Chem. Soc.* 121 (1999) 10119–10125.
- [7] J. Boyd, C. Redfield, Characterization of ^{15}N chemical shift anisotropy from orientation-dependent changes to ^{15}N chemical shifts in dilute bicelle solutions, *J. Am. Chem. Soc.* 121 (1999) 7441–7442.
- [8] W.Y. Choy, M. Tollinger, G.A. Mueller, L.E. Kay, Direct structure refinement of high molecular weight proteins against residual dipolar couplings and carbonyl chemical shift changes upon alignment: an application to maltose binding protein, *J. Biomol. NMR* 21 (2001) 31–40.
- [9] J.A.M.T.C. Cromsigt, C.W. Hilbers, S.S. Wijmenga, Prediction of proton chemical shifts in RNA – their use in structure, refinement, and validation, *J. Biomol. NMR* 21 (2001) 11–29.
- [10] J. Kuszewski, A.M. Gronenborn, M. Clore, The impact of direct refinement against proton chemical shifts on protein structure determination by NMR, *J. Magn. Reson. B* 107 (1995) 293–297.
- [11] N. Tjandra, A. Bax, Direct measurement of distances and angles in biomolecules by NMR in a dilute liquid crystalline medium, *Science* 278 (1997) 1111–1114.
- [12] J.H. Prestegard, H.M. al-Hashimi, J.R. Tolman, NMR structures of biomolecules using field oriented media and residual dipolar couplings, *Quart. Rev. Biophys.* 33 (2000) 371–424.
- [13] M. Suzuki, R.J. Youle, N. Tjandra, Structure of Bax: coregulation of dimer formation and intracellular localization, *Cell* 103 (2000) 645–654.
- [14] R.S. Lipsitz, N. Tjandra, Carbonyl CSA restraints from solution NMR for protein structure refinement, *J. Am. Chem. Soc.* 123 (2001) 11065–11066.
- [15] M.R. Hansen, L. Mueller, A. Pardi, Tunable alignment of macromolecules by filamentous phage yields dipolar coupling interactions, *Nat. Struct. Biol.* 5 (1998) 1065–1074.
- [16] E. de Alba, M. Suzuki, N. Tjandra, Simple multidimensional NMR experiments to obtain different types of one-bond dipolar coupling simultaneously, *J. Biomol. NMR* 19 (2001) 63–67.
- [17] D.S. Garrett, R. Powers, A.M. Gronenborn, G.M. Clore, A common sense approach to peak picking in two-, three-, and four-dimensional spectra using automatic computer analysis of contour diagrams, *J. Magn. Reson.* 95 (1991) 214–220.
- [18] A.C. Wang, A. Bax, Determination of the backbone dihedral angles ϕ in human ubiquitin from reparametrized empirical Karplus equations, *J. Am. Chem. Soc.* 118 (1996) 2483–2494.
- [19] G. Cornilescu, A. Bax, Measurement of proton, nitrogen, and carbonyl chemical shielding anisotropies in a protein dissolved in a dilute liquid crystalline phase, *J. Am. Chem. Soc.* 122 (2000) 10143–10154.
- [20] N. Tjandra, S. Grzesiek, A. Bax, Magnetic field dependence of nitrogen–proton J splittings in ^{15}N -enriched human ubiquitin resulting from relaxation interference and residual dipolar coupling, *J. Am. Chem. Soc.* 118 (1996) 6264–6268.
- [21] K. Pervushin, R. Riek, G. Wider, K. Wuthrich, Attenuated T_2 relaxation by mutual cancellation of dipole–dipole coupling and chemical shift anisotropy indicates an avenue to NMR structures of very large biological macromolecules in solution, *Proc. Natl. Acad. Sci. USA* 94 (1997) 12366–12371.
- [22] C.D. Schwieters, J.J. Kuszewski, N. Tjandra, G.M. Core, The Xplor-NIH NMR molecular structure determination package, *J. Magn. Reson.* 160 (2003) 65–73.
- [23] A.C. de Dios, J.G. Pearson, E. Oldfield, Secondary and tertiary structural effects on protein NMR chemical shifts: an ab initio approach, *Science* 260 (1993) 1491–1496.

- [24] J.R. Brender, D.M. Taylor, A. Ramanoorthy, Orientation of amide-nitrogen-15 chemical shift tensors in peptides: a quantum chemical study, *J. Am. Chem. Soc.* 123 (2001) 914–922.
- [25] J.C. Facelli, R.J. Pugmire, D.M. Grant, Effects of hydrogen bonding in the calculation of ^{15}N chemical shift tensors: benzamide, *J. Am. Chem. Soc.* 118 (1996) 5488–5489.
- [26] A. Shoji, S. Ando, S. Kuroki, I. Ando, G.A. Webb, Structural studies of peptides and polypeptides in the solid state by nitrogen-15 NMR, *Annu. Rep. NMR Spectrosc.* 26 (1993) 55–98.
- [27] S. Kuroki, S. Ando, I. Ando, A. Shoji, T. Ozaki, G.A. Webb, Hydrogen-bonding effect on N-15 chemical-shifts of the glycine residue of oligopeptides in the solid-state as studied by high-resolution solid-state NMR spectroscopy, *J. Mol. Struct.* 240 (1990) 19–29.